COMMUNICATIONS PHYSICS

ARTICLE

DOI: 10.1038/s42005-018-0059-7 OPEN

A high electron mobility phonotransistor

Caroline L. Poyser[1], Lianhe H. Li[2], Richard P. Campion[1], Andrey V. Akimov[1], Edmund H. Linfield[2], A. Giles Davies[2], John E. Cunningham[2] & Anthony J. Kent[1]

Acoustoelectric devices convert acoustic energy to electrical energy and vice versa. Devices working at much higher acoustic frequencies than those currently available have potential scientific and technological applications, for example, as detectors in phononics experiments and as transducers in bulk acoustic wave filters at terahertz (THz) frequencies. Here we demonstrated an active acoustoelectronic device based on a GaAs heterostructure: an acoustically gated transistor or phonotransistor. Instead of being controlled in the conventional manner by an electrical signal applied to a metallic or semiconductor gate as in a high electron mobility transistor (HEMT), the drain-source current was controlled by a bulk sub-THz acoustic wave passing through the channel in a direction perpendicular to the current flow.

[1] School of Physics and Astronomy, University of Nottingham, Nottingham NG7 2RD, UK. [2] School of Electronic and Electrical Engineering, University of Leeds, Leeds LS2 9JT, UK. Correspondence and requests for materials should be addressed to A.J.K. (email: anthony.kent@nottingham.ac.uk)

The ability to generate beams of coherent acoustic phonons by ultrafast pulsed laser excitation of nanometre-thickness metal or semiconductor films, first demonstrated in the 1980s[1,2], has given birth to the field of phononics research. In subsequent decades, the techniques have been refined such that the generation of picosecond-duration bursts of coherent phonons containing phonon frequencies up to a few hundred GHz is now well established; for a review see ref. [3]. Applications of these coherent phonons include: fundamental studies of phonon transport and interactions in materials;[3–7] hypersonic probing of nanostructures[8–10] and single biological cells[11,12] with nanometre resolution; control of the optical, electronic and magnetic properties of materials and devices;[13–15] and generation and detection of sub-THz electromagnetic radiation[16,17].

In phononics experiments, the detection of the coherent phonon bursts is indirect. The most common method, used in many of the works cited above, is through the acoustic modulation of the intensity of a transmitted or reflected light beam which is detected on a photodiode. Detection of the coherent phonon pulses through their heating effect, using bolometers, has also been demonstrated[18]. For a number of applications, it is desirable to have a device which converts the strain field associated with the coherent phonons directly into an electrical signal. Such devices are the phononic equivalent of photodiodes and phototransistors, which are considered essential components in the field of photonics. For a recent review of work in this field see ref. [19].

Any of the devices in which the control of electronic transport by coherent phonons has been demonstrated, e.g., Schottky diodes[13], resonant tunnelling diodes[20] and superlattices[21], could form the basis of a "phonodiode" detector. However, these devices have no capacity for gain, and the development of a "phonotransistor" with the potential for a gain effect has the potential to not only improve the sensitivity of phonon detection but also to facilitate the integration of coherent phonon signals into electrical circuits. To achieve the creation of a phonotransistor, this work investigates coherent phonon effects in high electron mobility transistors (HEMTs) based on the two-dimensional electron gas (2DEG) formed in a semiconductor heterojunction. These devices are interesting for terahertz (THz) phonon applications because they have been shown to work at high frequencies. An amplifier circuit based on HEMT devices holds the Guinness world record for the highest frequency amplifier, having been shown to measure at a gain of 9 decibels at 1 THz[22].

Acoustically driven electron transport in two-dimensional (2D) electron systems has been previously demonstrated, using surface acoustic waves (SAW) travelling parallel to the 2D layer[23–25]. In these experiments, the SAW, via the piezoelectric interaction, modulates the electric potential felt by the electrons, which become trapped in the potential minima and are "dragged" along with the SAW giving rise to the signals. It is also possible for the vertical component of SAW waves to be used for the control of vertical transport devices such as resonant tunnelling diodes[26]. These measurements are limited to frequencies of the order of a few GHz owing to the transducers used and SAW attenuation. Bulk acoustic waves have higher frequencies, but cannot be easily propagated parallel to a conventional 2DEG which is located only about 100 nm from the semiconductor surface.

In this paper, we show that we can control the lateral electron transport in a 2DEG device using bulk acoustic waves, of frequencies of tens to hundreds of GHz and propagating in a direction perpendicular to the plane of the 2DEG. We consider the physical process giving rise to the observed effects, and the factor(s) determining the speed of the measured response. We discuss potential phononics applications for the device, which we call a high electron mobility phonotransistor.

Results

Experimental arrangement. The experimental arrangement is shown in Fig. 1a. The samples featured an electrically contacted 2DEG structure on one side of the substrate and an aluminium film opto-acoustic transducer on the opposite side. The transducer generated, via the thermoelastic effect, bipolar picosecond acoustic (strain) pulses and launched them into the GaAs substrate. A typical strain pulse excited in this way has duration of ~10 ps, containing frequency components up to ~100 GHz[27]. The strain pulses propagated across the substrate at the speed of longitudinal sound and were incident on the 2DEG, whereupon they caused a change in conductivity of the channel. To prevent the attenuation of the phonon signal as it passed through the substrate, experiments were performed at 5 K unless stated otherwise. Two samples will be discussed in this paper, and these were designed to be identical aside from the spacer layer between the doping and 2DEG regions, which was 40 nm in sample A and 20 nm in sample B. The general sample structure can be seen in Fig. 1b.

Acoustoelectric response of the 2DEG. The inset to Fig. 1c shows the transient response of sample B to an acoustic pulse created by a pump laser power of 4.5 mW, corresponding to a laser fluence of ~3.6 mJ cm^{-2}, on the aluminium transducer. The DC background current was removed by the action of the bias tee. The excitation spot was located directly opposite the centre of the 2DEG channel, mid-way between the contacts. The signals during the first 10 ns, the large spike at time $t = 0$ followed by a train of pulses of decaying amplitude, are due to stray laser light reaching the device and being detected by the photoelectric effect. After a time, $t = 71$ ns, there is a 122 μA spike due to the strain pulse. The main Fig. 1c shows the acoustoelectric signal in more detail for both polarities of bias at a magnitude of 500 mV and in the case of zero bias. It is seen that the acoustic response reverses when the bias polarity is reversed with $\Delta I(t) < 0$ for $V > 0$ and $\Delta I(t) > 0$ for $V < 0$. In the case of $V = 0$ the acoustic wave produces a negligible response. These results show the incident strain pulse causes an increase in resistance of the 2DEG channel. This could be due to the deformation potential associated with the strain modulating the electronic band structure, causing a depletion of the charges in the channel, in a similar way to applying a negative gate bias to a HEMT. Alternatively, the strain pulse could cause a decrease of mobility of the electrons in the channel through heating or electron–phonon scattering.

Dependence of the acoustoelectric signal on applied DC bias. Figure 2a shows the acoustoelectric signal as a function of the bias voltage applied to the device. The results in Fig. 2a are shown for sample B at a laser fluence of ~2.6 mJ cm^{-2}. The DC current–voltage (IV) characteristics of this device can be seen in Fig. 2b for comparison. The acoustoelectric response was measured at the peak of the acoustic pulse. It is seen that both the acoustic signal and the DC current reach saturation at similar values of bias. We attribute the saturation of the current in the channel at high electric fields to electron drift velocity saturation effects. In this regime, the electron mobility is dominated by optical phonon scattering and becomes a strong function of the drain-source electric field (bias). The fact that the acoustic signal has the same shape as the IV characteristics indicates that strain-induced depletion of the carriers is the main cause of the signal. If the signal was, instead, caused by changes in the mobility due to acoustic phonon scattering, we would expect a strong decrease in its amplitude in the regime where optical phonon scattering dominates. For sample A, the signal showed similar saturation effects at high bias, and was found to reach a similar magnitude at

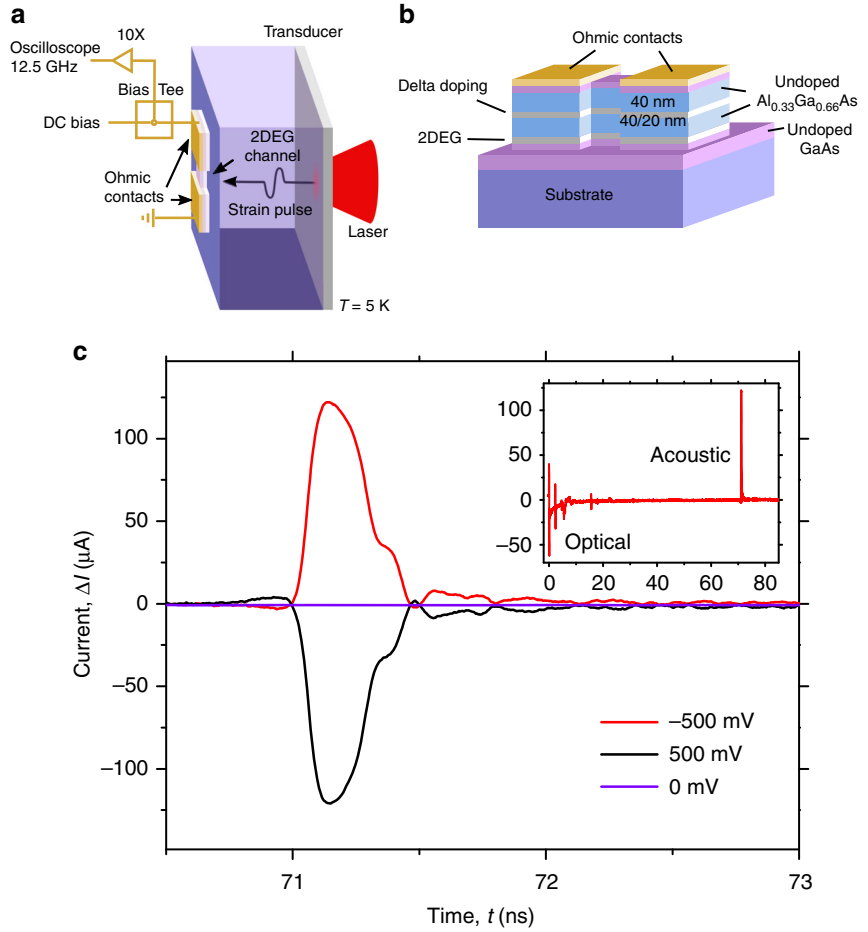

Fig. 1 Experiment details. **a** Schematic of experimental scheme. **b** Device structure, the delta-doped layer features a doping level of $n_d = 5.23 \times 10^{12}$ cm^{-2}. **c** Example of acoustic response of device. Signal recorded with sample B when the transducer film is excited with a laser fluence of 3.6 mJ cm^{-2}. The oscillations seen following the main signal peak are due to an electrical resonance caused by the filtering effect of the parasitic inductance and capacitance of the sample packaging

saturation, suggesting that the amplitude of the strain pulse is the main factor in determining signal magnitude rather than the specific device properties, such as mobility and carrier density.

Dependence of the acoustoelectric signal on strain amplitude. The amplitude of the strain pulse injected from the transducer is proportional to the pump laser fluence, and in Fig. 2c we show how the acoustoelectric response of the sample varies with pump fluence: We can see that both samples exhibit a highly non-linear increase of signal with pump fluence. We attribute this behaviour to the non-linear acoustic propagation effects that occur at high strain values, and the change in the spectrum of the acoustic pulse we expect at high strain powers. We see this non-linearity manifesting itself as a broadening of the electrical signal and its movement to earlier times, by about 180 ps between the lowest and highest pump powers, as can be seen in Fig. 2d. The movement to earlier times can only be explained by non-linear acoustic propagation effects which lead to a sharpening of the edges of the acoustic pulse whose leading edge travels at a speed which is slightly greater than the speed of sound in the linear regime[28–31]. Analysis of the signal arrival time shows that the maximum strain amplitudes generated in our measurements are in the mid 10^{-3} range. An important effect of acoustic non-linearity is the formation of strain components in the pulse that are much higher in frequency, up to ~1 THz, than present in the strain pulse initially generated in the Al transducer, ~100 GHz. The fact that signals are only detected in the devices at high strain amplitudes and the non-linear response in Fig. 2c implies that the device is more sensitive to strain pulses that have been modified by propagation in the acoustic non-linear regime.

Temperature dependence of acoustoelectric signal. Figure 2e shows the dependence of the acoustic signal on the temperature of the sample. For comparison, Fig. 2f shows the mobility of the samples measured as a function of temperature using a four-terminal measurement. If the cause of the acoustic signal is a change in the 2DEG carrier concentration, the temperature dependence of the signal would be expected to follow the temperature dependence of the mobility. While the signal does decrease with increasing temperature like the mobility, the decrease is faster, and the signal is negligible at temperatures above 70 K. This is probably due to attenuation of the higher frequency acoustic components as the temperature increases. At temperatures above about 50 K, the attenuation of phonons of frequency >200 GHz propagating across n~ 350 μm GaAs wafer becomes significant[7].

Simulation of the acoustoelectric response of 2DEG. Based on the results above, we propose that the observed response is due to the acoustic wave inducing a decrease in the 2DEG carrier density as it propagates through the heterostructure. Owing to the deformation potential coupling, the strain associated with the

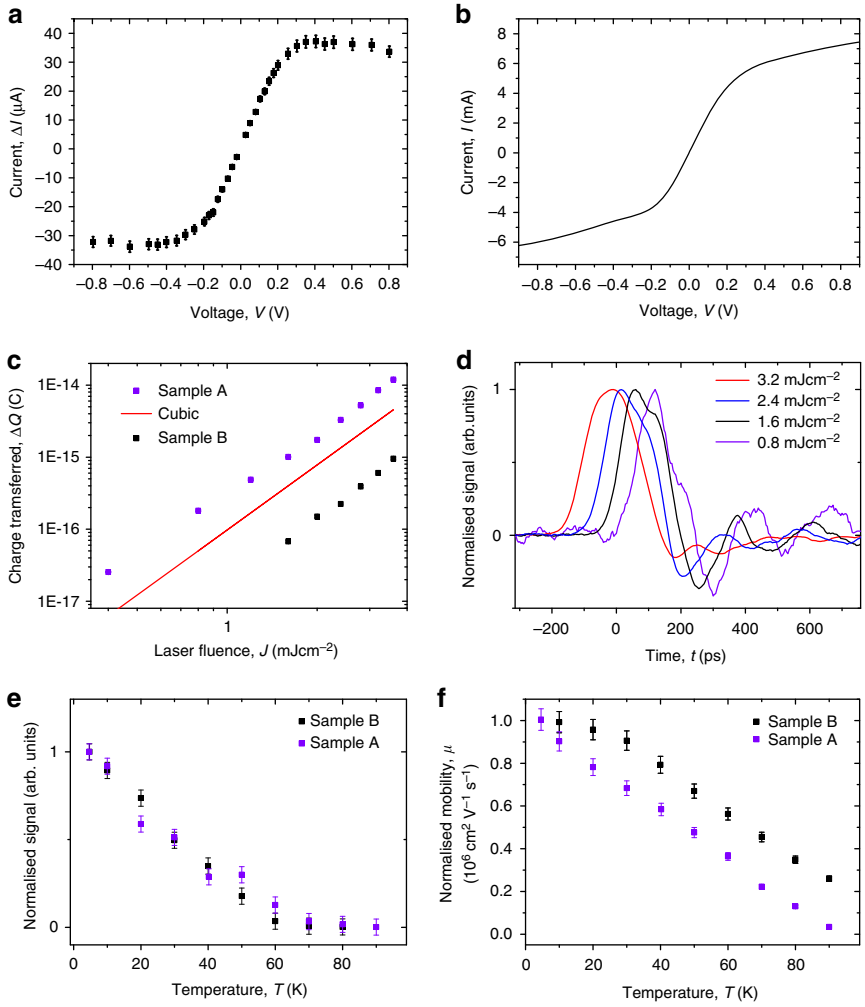

Fig. 2 Results. **a** Dependence of acoustic signal on sample B on bias. Signal taken using an exciting laser fluence on the transducer film of 2.5 mJ cm^{-2}. **b** IV characteristic of sample B at 5 K. **c** Dependence of acoustic signal in both samples on the laser fluence incident on the transducer film. Signals on sample A were taken with 500 mV of bias applied to the device, while for sample B 100 mV was applied. **d** Temporal shift of the signals measured on sample B at 100 mV. **e** Dependence of acoustic signal on sample temperature. **f** Sample mobility as a function of temperature measured using a four-point method; the signals have been normalised to the mobility of sample A. Error bars were all estimated from the standard deviation of a repeated measurement

acoustic wave shifts the energy bands. This shift in the relative energies of the 2DEG layer and the doped AlGaAs layer causes a transfer of electrons between the two and hence a change in the conduction of the 2DEG. The deformation potential associated with the strain therefore has a similar effect to applying an electrical gate signal to the device. The conduction band deformation potential is negative in Ga(Al)As, and hence the compressional (negative strain) part of the acoustic wave causes an increase in the band energy and the tensional (positive strain) part causes a decrease in the band energy. The relative shift in the energies between the 2DEG inversion layer and the doped layer causes a transfer of electrons and hence a change in the conductivity of the 2DEG.

We have simulated the effect of a bipolar strain pulse moving through the two regions of interest, the delta-doped layer and the 2DEG layer, taking account of non-linear acoustic propagation using the Burgers equation[32]. Referring to Fig. 3a we see that as the acoustic wave moves up through the structure, the first region of interest it encounters is the 2DEG. It will travel through this and reach the doped layer after a time equal to $t_1 = \frac{d_d}{S_{AlGaAs}}$, where d_d is the thickness of the spacer between the doped region and the 2DEG and S_{AlGaAs} is the speed of sound in $Al_{0.33}Ga_{0.67}As$ at low temperatures = 5031 ms^{-1}. After moving beyond the dopant region, the strain pulse continues to travel to the sample surface from which it is reflected, with a phase reversal, back through the structure. The strain pulse then re-encounters the doped region after a time equal to $t_2 = \frac{2d_s}{S_{AlGaAs}}$ where d_s is the distance to the surface and the other symbols are as before, after which the strain passes the 2DEG region again. By superposition of the effect of the forward and reflected strain pulse on the relative levels of the 2DEG compared to the doped layer, we can simulate how the band structure of the sample will be shifted over time. An example of this simulation can be seen in Fig. 3b. We modelled the strain as having an asymmetric effect on the signal, only considering the effect of potential shifts between the energy levels in the 2DEG and doping layer which would result in a depletion of carriers in the channel. This is consistent with the acoustic wave causing an increase in the resistance of the device as seen experimentally. The assumption of an asymmetric device response is reasonable as a gated device fabricated from a similar structure was found to work only in depletion mode. To allow comparison between the simulation and the measured signal, we applied a fourth-order Butterworth filter with a 3 GHz cut-off to the simulation. This accounts for the effect of the finite electrical

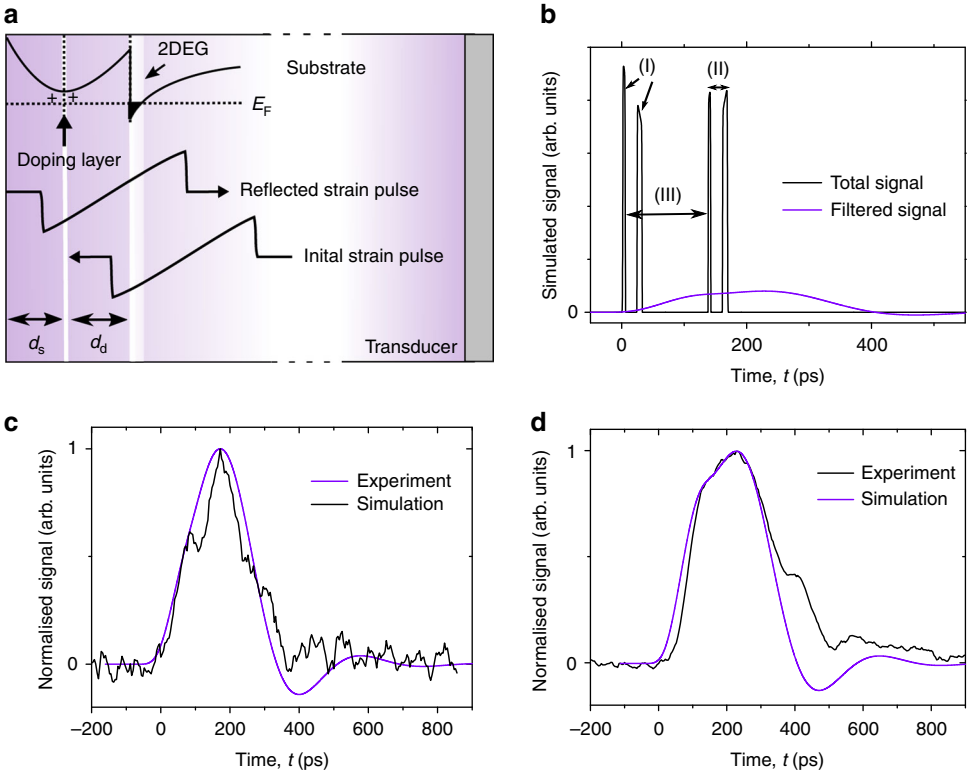

Fig. 3 Simulations. **a** Schematic of strain travelling through the structure. **b** Example of the signal expected due to the combined effect of the forward and reflected strain pulses moving through the structure. The width of the peaks seen, labelled I, is related to d_d the distance between the doping and the 2DEG layer, time II is related to the time it takes the strain to travel to the surface and reflect from the 2DEG layer, while the time III is related to the width of the strain pulse. The signal is shown before and after filtering. Comparison of samples measured using sample B and simulated in the case when the transducer film was excited with a laser fluence of **c** 3.6 mJ cm^{-2} and **d** 2 mJ cm^{-2}. The simulation parameters can be found in the text for both these figures

bandwidth of the sample packaging, cabling and measurement electronics. Figure 3c shows a comparison of the signal measured with sample B using a pump fluence of ~3.6 mJ cm^{-2}. A strain level of 1.5×10^{-3} and an initial pulsewidth, before non-linear propagation, of ~10 ps peak to peak were used. The best match of the modelled response to the measured signal was obtained by assuming the percentage of strain reflected from the surface was ~90% implying a small loss of signal due to scattering at the surface. Figure 3d shows a simulation of a signal taken when sample B was excited with a lower pump fluence, and for this signal an initial strain value of 8×10^{-4} was used but otherwise all parameters were as for Fig. 3c.

Discussion

Measurements of the dependence of the acoustically induced signal on the pump fluence and the temperature both pointed to the 2DEG being most sensitive to the acoustic waves of frequency >150 GHz. We see this is consistent with the proposed model and simulations. So that the strain causes a relative shift of the band energies and hence transfer of charge between the 2DEG and the donor levels, the acoustic wavelength must be smaller than the thickness of the spacer layer between the doped layer and the 2DEG. Acoustic waves having much larger wavelengths do not cause a relative shift of the band energies of the 2DEG and doped layer, and so cause no charge transfer, and hence induce no signal. For sample A, therefore, a low frequency cut-off occurs at $f_c \approx S_{AlGaAs}/2d_d \approx 63$ GHz, and for sample B at around 126 GHz. Previous work suggests that in the linear acoustic regime the frequencies generated by a 30 nm aluminium film such as used in this work extend to ~100 GHz[27], and so our device sensitivities are on the limit of what is achievable in the linear regime and this is why we only observed clear signals in the non-linear acoustic regime.

The typical magnitude of the strain in our experiments is $\mathcal{E}$ ~10^{-3}, and the magnitude of the deformation potential in GaAs, Ξ_D is about 10 eV per unit strain[33]. Therefore, the acoustically induced potential change in the structure is $\varepsilon \Xi_D$ ~10 mV. The measured signal amplitude at the terminals of the device in a load of 50 Ω is of order one millivolt. However, a fourth-order filter with a 3 GHz cut-off frequency would attenuate a signal of frequency corresponding to the phonon pulse by a factor of ~100×, and therefore we deduce that the acoustically induced signal amplitude must be of order 100 mV, which implies the device possesses an acoustoelectric "gain" or "transistor" action.

It is interesting to do a rough comparison between the sensitivity of the phonotransistor and a conventional all-optical pump–probe experiment. In a typical pump–probe experiment, where changes of the reflectance of a laser probe beam are used to measure the phonons, the level of reflectivity changes $\left(\frac{\Delta R}{R}\right)$ are typically in the order of 10^{-5} as in ref. [3]. Assuming a laser power level in the reflected probe beam of 10 mW, we would therefore expect a signal due to the reflectivity change of ~0.1 μW. If we detect this using a standard silicon photodiode which produces an output of around 0.5 A W^{-1}, we expect currents in the range of a hundred nano amps, around a thousand times less than signals measured in the phonotransistor.

In summary, we have demonstrated that an acoustic wave normally incident on a 2DEG can induce a change in the electrical current. We find that the device has a high sensitivity to the acoustic waves owing to the transistor (gain) effect, and we offer a qualitative explanation for the effect due to the deformation potential action of the acoustic wave on the energy bands of the

structure. 2DEG structures have been heavily researched in the THz community with novel structures being designed as plasmon emitters (for a review see ref. [34]). A potential route for future investigation is using acoustic waves to modify the carrier concentration in these structures providing the possibility for fast modulation of the signals in these devices. Phonotransistors also have a great potential to provide fast electrical detection of the acoustic waves with comparatively simple manufacturing requirements compared to other high-frequency devices. Although our electrical measurement is limited to frequencies <~10 GHz, our results suggest that the 2DEG device is sensitive to acoustic waves with frequencies extending significantly up above 150 GHz. Therefore, such a 2DEG could be used to convert coherent acoustic waves to THz radiation.

Methods

Sample structures. The experimental arrangement is shown in Fig. 1a: GaAs/AlGaAs heterojunction 2DEG structures were grown by molecular beam epitaxy on approximately 0.5 mm-thick semi-insulating GaAs substrates. Two samples will be discussed in this paper, and these were designed to be identical aside from the spacer layer between the doping and 2DEG regions, which was 40 nm in sample A and 20 nm in sample B. The structures, shown in Fig. 1b, consisted of: a 1.3 μm GaAs buffer layer; a 40 nm (sample A) or 20 nm (sample B) $Al_{0.33}Ga_{0.67}As$ spacer; a layer of $Al_{0.33}Ga_{0.67}As$, delta doped with Si to ~5×10^{12} cm^{-2}; 40 nm of $Al_{0.33}Ga_{0.67}As$; and a 17 nm GaAs top cap. The areal carrier density, n_s, of the two samples was measured using Shubnikov de Haas oscillations at approximately 4 K. Sample A (40 nm spacer) had $n_s = (1.94 \pm 0.01) \times 10^{11}$ cm^{-2} while sample B (20 nm spacer) had $n_s = (3.9 \pm 0.02) \times 10^{11}$ cm^{-2}. The low-field mobilities, μ, of the two samples at 10 K measured using a four-terminal method were found to be: for sample A, $\mu = (1.00 \pm 0.05)$ x 10^6 cm^2 V^{-1} s^{-1} and for sample B, $\mu = 450{,}000 \pm 20{,}000$ cm^2 V^{-1} s^{-1}. A Mesa etch defined the 2DEG channel which had dimensions of ≈120 μm by 95 μm and GeAuNi Ohmic source and drain contacts were made at each end.

Experimental details. On the back side of the substrate, opposite to the 2DEG device, a 30 nm-thick Al opto-acoustic transducer film was deposited. The Al transducer was pumped with femtosecond pulses from an amplified Ti:Sapphire laser (pulsewidth = 85 fs; wavelength = 800 nm; repetition rate = 5 kHz; and maximum energy = 1 mJ). The device had a DC bias applied to it, using a microwave bias tee, and the signal response was detected on a 12.5 GHz bandwidth digital oscilloscope.

The laser spot size used to excite the transducer varied slightly between datasets due to differences in the experimental arrangement, and hence in the Results section, an estimation of the fluence of the exciting laser pulse is given, based on an estimation of the expected spot size in each focussing arrangement.

Data availability

The datasets generated during and/or analysed during the current study are available from the corresponding author on reasonable request.

Received: 6 March 2018 Accepted: 24 August 2018
Published online: 28 September 2018

References

1. Grahn, H. T., Maris, H. J., & Tauc, J. Picosecond ultrasonics. *IEEE J. Quantum. Electron.* **25**, 2562–2569 (1989).
2. Thomsen, C., Grahn, H. T., Maris, H. J. & Tauc, J. Surface generation and detection of phonons by picosecond light pulses. *Phys. Rev. B* **34**, 4129–4138 (1986).
3. Péronne, E., & Perrin, B. Ultrafast acoustics. *Ultrasonics* **56**, 1–576 (2015).
4. Dehoux, T. et al. Optical tracking of picosecond coherent phonon pulse focusing inside a sub-micron object. *Light Sci. Appl.* **5**, e16082 (2016).
5. van Capela, P. J. S., Péronne, E. & Dijkhuisa, J. I. Nonlinear ultrafast acoustics at the nano scale. *Ultrasonics* **56**, 36–51 (2015).
6. Volz, S. et al. Nanophononics: state of the art and perspectives. *Eur. Phys. J. B* **89**, 15 (2016).
7. Legrand, R., Huynh, A., Jusserand, B., Perrin, B. & Lemaitre, A. Direct measurement of coherent subterahertz acoustic phonons mean free path in GaAs. *Phys. Rev. B* **93**, 184304 (2016).
8. Dehoux, T., Wright, O. B., Voti, R. L. & Gusev, V. E. Nanoscale mechanical contacts probed with ultrashort acoustic and thermal waves. *Phys. Rev. B* **80**, 235409 (2009).
9. Mante, P.-A., Huang, Y.-R., Yang, S.-C., Liu, T.-M. & Maznev, A. A. THz acoustic phonon spectroscopy and nanoscopy by using piezoelectric semiconductor heterostructures. *Ultrasonics* **56**, 52–65 (2015).
10. Jean, C. et al. Spatiotemporal imaging of the acoustic field emitted by a single copper nanowire. *Nano Lett.* **16**, 6592–6598 (2016).
11. Gadalla, A., Dehoux, T. & Audoin, B. Transverse mechanical properties of cell walls of single living plant cells probed by laser-generated acoustic waves. *Planta* **239**, 1129–1137 (2014).
12. Dehoux, T. & Audoin, B. Non-invasive optoacoustic probing of the density and stiffness of single biological cells. *Appl. Phys. Lett.* **12**, 124702 (2012).
13. Moss, D. M., Akimov, A. V., Glavin, B. A., Henini, M. & Kent, A. J. Ultrafast strain-induced current in a GaAs Schottky diode. *Phys. Rev. Lett.* **106**, 066602 (2011).
14. Czerniuk, T. et al. Impact of nanomechanical resonances on lasing from electrically pumped quantum dot micropillars. *Appl. Phys. Lett.* **106**, 041103 (2015).
15. Kats, V. N. et al. Ultrafast changes of magnetic anisotropy driven by laser-generated coherent and noncoherent phonons in metallic films. *Phys. Rev. B* **93**, 214422 (2016).
16. Heywood, S. L. et al. Heterodyne mixing of millimetre electromagnetic waves and sub-THz sound in a semiconductor device. *Sci. Rep.* **6**, 30396 (2016).
17. Armstrong, M. R., Reed, E. J., Kim, K.-Y., Glownia, J. H. & Howard, W. M. Observation of terahertz radiation coherently generated by acoustic waves. *Nat. Phys.* **5**, 285–288 (2009).
18. Stanton, N. M. & Kent, A. J. Propagation of high amplitude strain pulses in sapphire. *Phys. Rev. B* **73**, 220301 (2006).
19. Akimov, A. V., Poyser, C. L. & Kent, A. J. Review of microwave electro-phononics in semiconductor nanostructures. *Semicond. Sci. Technol.* **32**, 053003 (2017).
20. Young, E. S. K., Akimov, A. V., Henini, M., Eaves, L. & Kent, A. J. Subterahertz acoustical pumping of electronic charge in a resonant tunneling device. *Phys. Rev. Lett.* **108**, 226601 (2012).
21. Poyser, C. L., Akimov, A. V., Balanov, A. G., Campion, R. P. & Kent, A. J. A weakly coupled semiconductor superlattice as a harmonic hypersonic-electrical transducer. *New J. Phys.* **17**, 083064 (2015).
22. Mei, X. et al. First demonstration of amplification at 1 THz using 25-nm InP high electron mobility transistor process. *IEEE Electron Device Lett.* **36**, 327–329 (2015).
23. Talyanskii, V. I. et al. Quantized current in one-dimensional channel induced by surface acoustic waves. *Phys. B Condens. Matter* **249**, 140–146 (1998).
24. Shilton, J. M. et al. High-frequency single-electron transport in a quasi-one-dimensional GaAs channel induced by surface acoustic waves. *J. Phys. Condens. Matter* **8**, L531 (1996).
25. Sogawa, T. et al. Photoluminescence dynamics of GaAs/AlAs quantum wells modulated by surface acoustic waves. *Jpn. J. Appl. Phys.* **46**, L758 (2007).
26. Hutchinson, A. B. et al. Nonlinear interaction between surface acoustic waves and electrons in GaAs resonant-tunneling structures. *Phys. Rev. B* **62**, 6948 (2000).
27. Young, E. S. K., Akimov, A. V., Campion, R. P., Kent, A. J. & Gusev, V. Picosecond strain pulses generated by a supersonically expanding electron-hole plasma in GaAs. *Phys. Rev. B* **86**, 155207 (2012).
28. Hao, H.-Y. & Maris, H. J. Experiments with acoustic solitons in crystalline solids. *Phys. Rev. B* **64**, 064302 (2001).
29. Scherbakov, A. V. et al. Chirping of an optical transition by an ultrafast acoustic soliton train in a semiconductor quantum well. *Phys. Rev. Lett.* **99**, 057402 (2007).
30. Péronne, E. & Perrin, B. Generation and detection of acoustic solitons in crystalline slabs by laser ultrasonics. *Ultrasonics* **44**, e1203–e1207 (2006).
31. Péronne, E., Chuecos, N., Thevenard, L. & Perrin, B. Acoustic solitons: a robust tool to investigate the generation and detection of ultrafast acoustic waves. *Phys. Rev. B* **95**, 064306 (2017).
32. Karpman, V. I. *Non-Linear Waves in Dispersive Media: International Series of Monographs in Natural Philosophy* (Pergamon Press, Oxford, 1975).
33. Vurgaftman, I., Meyer, J. R. & Ram-Mohan, L. R. Band parameters for III-V compound semiconductors and their alloys. *J. Appl. Phys.* **89**, 5815–5875 (2001).
34. Otsuji, T. et al. Emission and detection of terahertz radiation using two-dimensional plasmons in semiconductor nanoheterostructures for nondestructive evaluations. *Opt. Eng.* **53**, 031206–031206 (2014).

Acknowledgements

This work was supported by the Engineering and Physical Sciences Research Council (grant numbers EP/M016161/1, EP/M01598X/1, EP/P021859/1), and the U.S. Army Research Laboratory (Grant Number W911NF-14-1-0586). E.H.L. and A.G.D. are grateful for support from the Royal Society and the Wolfson Foundation. The authors would also like to thank Mr. M. Young for assistance in performing Shubnikov de Haas oscillation measurements.

Author contributions

A.J.K. and C.L.P. developed the idea for the experiment; C. L. P., A.V.A. and A.J.K. performed the experiment; C.L.P., A.V.A. and A.J.K. analysed the experimental data; E.H. L., L.H.L. and R.P.C were responsible for wafer growth using molecular beam epitaxy; C. L.P. fabricated the samples; C.L.P., A.J.K., A.V.A., A.G.D. and J.E.C. wrote the manuscript; A.J.K., J.E.C., A.G.D. and E.H.L. conceived and organised the project.

Additional information

Competing interests: The authors declare no competing interests.

Reprints and permission information is available online at http://npg.nature.com/reprintsandpermissions/

Publisher's note: Springer Nature remains neutral with regard to jurisdictional claims in published maps and institutional affiliations.